Supplementary Information to:

Unraveling the mechanism of biomimetic hydrogen fuel production - A first principles molecular dynamics study

Rakesh C. Puthenkalathil, Mihajlo Etinski, and Bernd Ensing

1 Gas phase geometry optimisation

Figures 1a and 1b show the results of electronic energy calculations of complexes **1** and $\mathbf{1}^-$ using three different functional/basis-set combinations (PBE/DZVP, PBE/TZV2P, and BLYP/TZV2P) at different electronic spin multiplicities (M=2S+1). All three combinations predict the correct trend of the relative energies. The DZVP and TZV2P basis sets predict almost equal values for the relative energy using the PBE functional. The low-spin state is the ground-state for this complex, in agreement with previous studies[1,2]. Hence, in our DFT-MD simulations, multiplicities of 1 and 2 are used for the closed shell and open shell systems respectively.

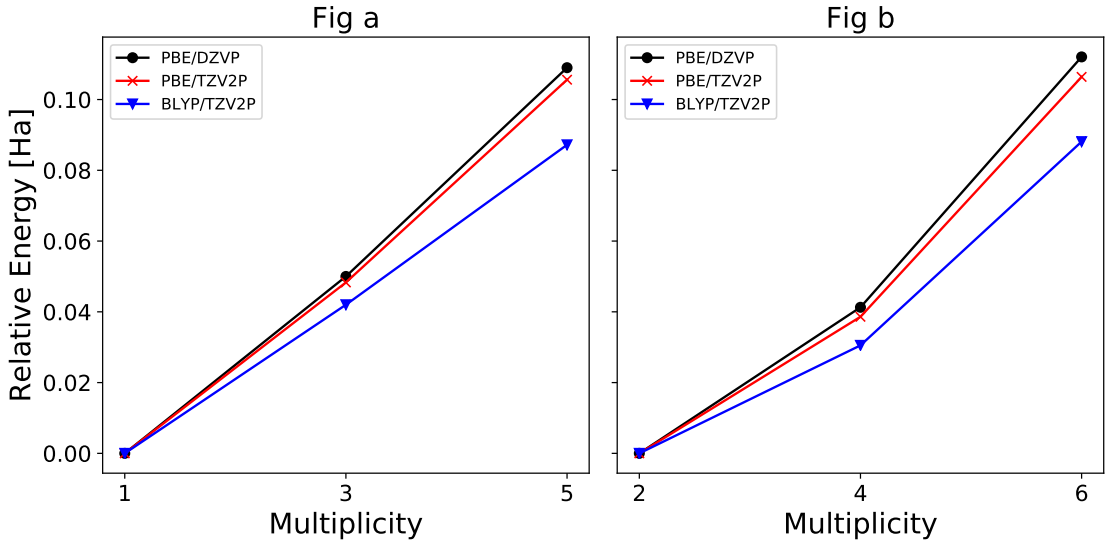

Figure 1: Relative energies of complex **1** (Fig. a) and complex $\mathbf{1}^-$ (Fig b) at different multiplicities for three combinations of XC functional and basis set.

Tables 1-3 and Tables 4-6 shows the bond lengths of Fe-Fe and Fe-S using different functional/basis set combinations for the **1** and $\mathbf{1}^-$ complexes, respectively. See Figure 2 for the atom labeling. Based on these calculations, we chose the PBE/DZVP level of theory for the DFT-MD calculations. See also Ref. 3 for a detailed analysis of static DFT calculations on these systems.

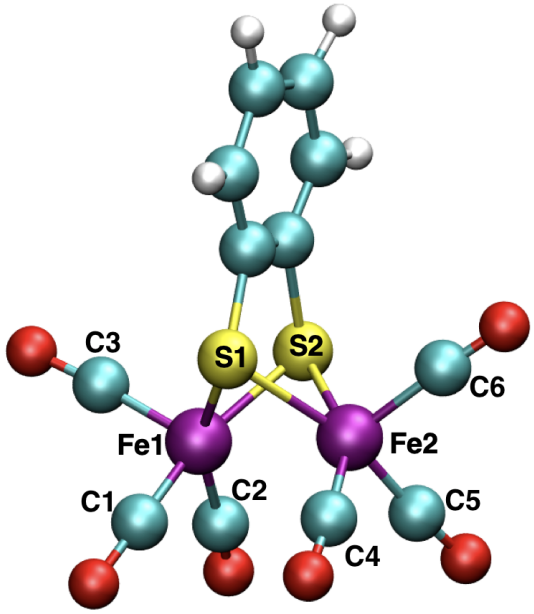

Figure 2: Atom labels (as used in Tables 1 to 6) indicated at the hand of the molecular structure of complex **1**.

Multiplicity	Fe1-Fe2	Fe1-S1	Fe1-S2	Fe2-S1	Fe2-S2
1	2.49	2.28	2.28	2.29	2.28
3	2.56	2.22	2.25	3.38	2.26
5	3.18	2.23	2.26	3.67	2.28

Table 1: Selected optimized bond lengths (in Å) calculated using PBE/DZVP for complex **1**.

Multiplicity	Fe1-Fe2	Fe1-S1	Fe1-S2	Fe2-S1	Fe2-S2
1	2.5	2.28	2.28	2.28	2.28
3	2.57	2.22	2.25	3.37	2.26
5	3.18	2.23	2.26	3.71	2.28

Table 2: Selected optimized bond lengths (in Å) calculated using PBE/TZV2P for complex **1**.

Multiplicity	Fe1-Fe2	Fe1-S1	Fe1-S2	Fe2-S1	Fe2-S2
1	2.5	2.28	2.28	2.28	2.28
3	2.65	2.27	2.29	3.46	2.29
5	3.35	2.27	2.31	3.91	2.30

Table 3: Selected optimized bond lengths (in Å) calculated using BLYP/TZV2P for complex **1**.

Multiplicity	Fe1-Fe2	Fe1-S1	Fe1-S2	Fe2-S1	Fe2-S2
2	2.51	2.33	2.33	2.37	2.37
4	3.31	2.27	2.27	2.29	4.03
6	3.10	2.26	3.09	2.26	3.11

Table 4: Selected optimized bond lengths (in Å) calculated using PBE/DZVP for complex $\mathbf{1}^-$.

Multiplicity	Fe1-Fe2	Fe1-S1	Fe1-S2	Fe2-S1	Fe2-S2
2	2.54	2.32	2.28	2.33	2.55
4	3.32	2.28	2.27	2.30	4.06
6	3.09	2.27	3.08	2.27	3.12

Table 5: Selected optimized bond lengths (in Å) calculated using PBE/TZV2P for complex $\mathbf{1}^-$.

Multiplicity	Fe1-Fe2	Fe1-S1	Fe1-S2	Fe2-S1	Fe2-S2
2	2.64	2.39	2.29	2.29	3.25
4	3.52	2.32	2.32	2.33	4.18
6	3.56	2.2.8	3.26	2.28	3.39

Table 6: Selected optimized bond lengths (in Å) calculated using BLYP/TZV2P for complex $\mathbf{1}^-$.

2 Geometric parameters of complex 1 at different intermediate states

Tables 7 and 8 show the average bond lengths and the standard deviations (in Å) of selected bonds observed in the DFT-MD simulations at $T = 298$ K. In the 1H intermediate state, the Fe-Fe bond is elongated by 0.23 Å.

	1	$\mathbf{1}^{-}$	$\mathbf{1}^{2-}$
Fe1-Fe1	2.49 (± 0.26)	2.57 (± 0.17)	2.67 (± 0.15)
Fe1-S1	2.27 (± 0.24)	3.01 (± 0.24)	2.35 (± 0.12)
Fe1-S2	2.27 (± 0.24)	2.49 (± 0.21)	3.86 (± 0.25)
Fe2-S1	2.27 (± 0.24)	2.31 (± 015)	2.26 (± 0.09)
Fe2-S2	2.27 (± 0.24)	2.27 (± 0.15)	2.34 (± 0.12)
Fe1-C1	1.75 (± 0.18)	1.76 (± 0.12)	1.74 (± 0.06)
Fe1-C2	1.76 (± 0.18)	1.76 (± 0.11)	1.74 (± 0.06)
Fe1-C3	1.76 (± 0.19)	1.75 (± 0.11)	1.76 (± 0.06)
Fe1-C4	3.39 (± 0.37)	3.31 (± 0.28)	2.10 (± 0.30)
Fe1-C5	4.09 (± 0.38)	3.00 (± 0.31)	3.70 (± 0.26)
Fe1-C6	2.27 (± 0.42)	4.23 (± 0.26)	4.07 (± 0.20)
Fe2-C1	3.21 (± 0.36)	3.29 (± 0.28)	3.98 (± 0.20)
Fe2-C2	3.40 (± 0.38)	3.71 (± 0.40)	3.26 (± 0.29)
Fe2-C3	4.10 (± 0.42)	3.96 (± 0.38)	3.91 (± 0.22)
Fe2-C4	1.75 (± 0.18)	1.76 (± 0.11)	1.89 (± 0.10)
Fe2-C5	1.75 (± 0.18)	1.76 (± 0.12)	1.74 (± 0.06)
Fe2-C6	1.75 (± 0.19)	1.75 (± 0.11)	1.72 (± 0.06)

Table 7: Average bond lengths and (in parentheses) standard deviations (both in Å) of complex **1** in the oxidized, single reduced and doubly reduced states, obtained from the DFT-MD simulations at $T = 298$ K.

	1H	**1H$^-$**	**1H^{2-}**
Fe1-Fe1	2.72 (± 0.17)	2.57 (± 0.17)	2.58 (± 0.15)
Fe1-S1	2.34 (± 0.15)	2.34 (± 0.17)	2.31 (± 0.08)
Fe1-S2	2.37 (± 0.17)	2.27 (± 0.09)	2.31 (± 0.09)
Fe2-S1	2.35 (± 0.16)	3.92 (± 0.14)	4.11 (± 0.18)
Fe2-S2	2.36 (± 0.17)	2.36 (± 0.10)	3.86 (± 0.32)
Fe1-C1	1.77 (± 0.11)	1.75 (± 0.05)	1.83 (± 0.09)
Fe1-C2	1.77 (± 0.11)	1.86 (± 0.06)	1.88 (± 0.10)
Fe1-C3	1.80 (± 0.12)	1.73 (± 0.09)	1.73 (± 0.05)
Fe1-C4	3.69 (± 0.24)	3.53 (± 0.13)	3.71 (± 0.14)
Fe1-C5	3.77 (± 0.26)	3.93 (± 0.13)	3.75 (± 0.19)
Fe1-C6	4.24 (± 0.26)	3.77 (± 0.13)	3.69 (± 0.18)
Fe2-C1	3.68 (± 0.25)	3.61 (± 0.15)	2.93 (± 0.25)
Fe2-C2	3.79 (± 0.24)	2.09 (± 0.16)	2.13 (± 0.21)
Fe2-C3	4.24 (± 0.26)	4.08 (± 0.13)	3.91 (± 0.18)
Fe2-C4	1.76 (± 0.11)	1.75 (± 0.07)	1.77 (± 0.10)
Fe2-C5	1.76 (± 0.11)	1.76 (± 0.09)	1.76 (± 0.08)
Fe2-C6	1.79 (± 0.11)	1.79 (± 0.10)	1.76 (± 0.06)
Fe1-H	1.70 (± 0.14)	1.80 (± 0.12)	1.91 (± 0.19)
Fe2-H	1.68 (± 0.14)	1.62 (± 0.09)	1.60 (± 0.10)

Table 8: Average bond lengths and (in parentheses) standard deviations (both in Å) of the protonated complex **1** in the oxidized, single reduced and doubly reduced states, obtained from the DFT-MD simulations at $T = 298$ K.

Figures 3 and 4 show the changes in Fe-S bond lengths over time for the intermediate states $\mathbf{1}^-$ and $\mathbf{1}^{2-}$. The starting point of these simulations are the equilibrated neutral complex. At the $\mathbf{1}^-$ intermediate state, one of the Fe-S bonds is elongated. At the $\mathbf{1}^{2-}$ state, one Fe-S bond is broken and a rearrangement of the CO group is observed. This process is spontaneous and is observed within 1 ps of DFT-MD simulation time.

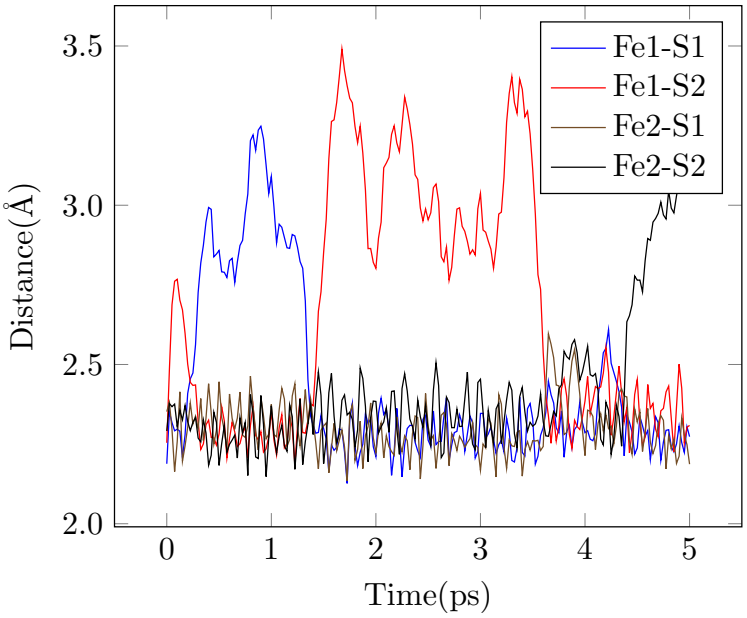

Figure 3: Fe-S bond lengths in complex $\mathbf{1}^{-}$. Alternating, one of the Fe-S bonds is elongated. All CO groups remains at terminal positions.

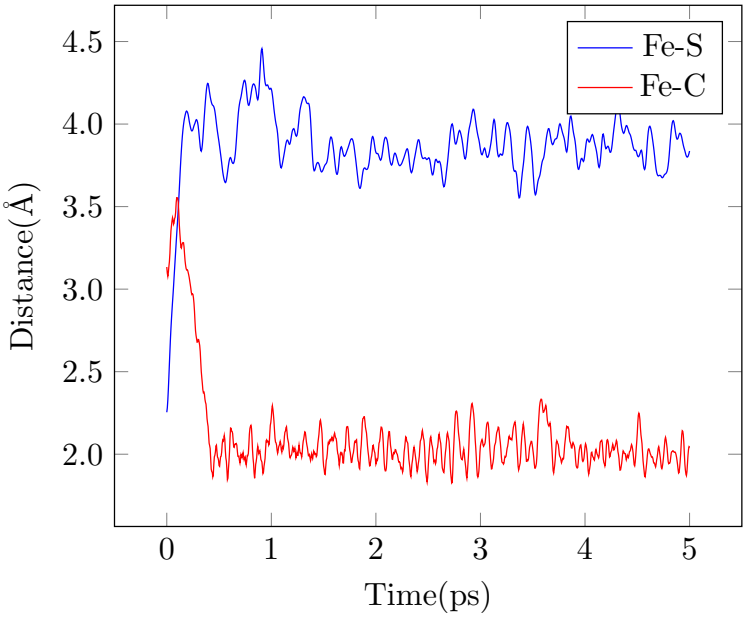

Figure 4: One Fe-S bond is seen to break quickly after two-electron reduction of the initial complex to form $\mathbf{1}^{2-}$. The Fe-S distance is stretched to almost 4 Å, while simultaneously a CO group rearranges to the bridging position.

3 S^2 values and Wannier centers positions in the spin-polarised complexes

Complexes $\mathbf{1}^-$, **1H**, and $\mathbf{1H}^{2-}$ have an unpaired electron (*i.e.* spin multiplicity 2). The average values for the expectation value of the total spin, S^2, in the DFT-MD simulations of these complexes were 0.771, 0.760, and 0.764, respectively, which is sufficiently close to the ideal number of 0.75, to consider spin contamination effects negligible.

Figures 4 and 5 in the main text show only the Wannier centers positions computed from the up-spin wave function. For completeness, here we show in Figure 5 also the Wannier center positions associated with the down-spin wave functions. Panels a, b, and c show these Wannier center positions in the complexes $\mathbf{1}^-$, **1H**, and $\mathbf{1H}^{2-}$, respectively. Formal oxidation states were calculated by adding the numbers of Wannier centers from both up and down spin states.

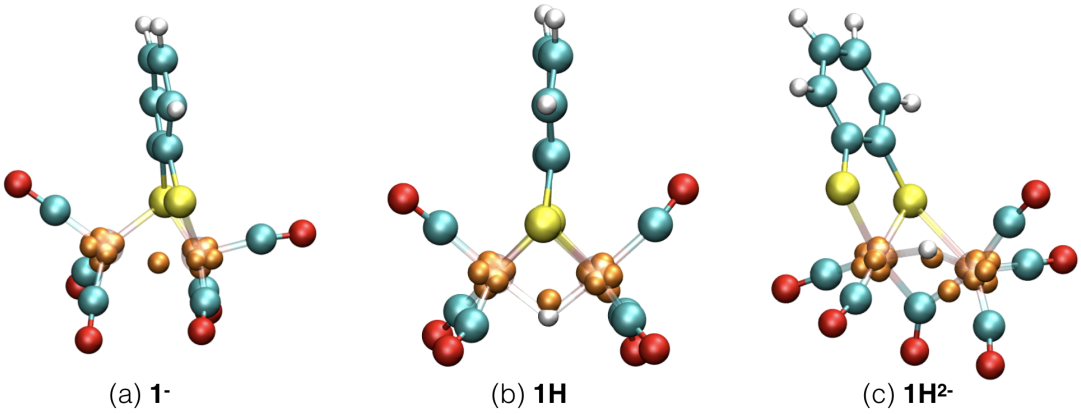

Figure 5: Wannier center positions computed from the down-spin wave functions of the spin-polarised intermediate complexes.

4 Side-view of the different intermediate structures

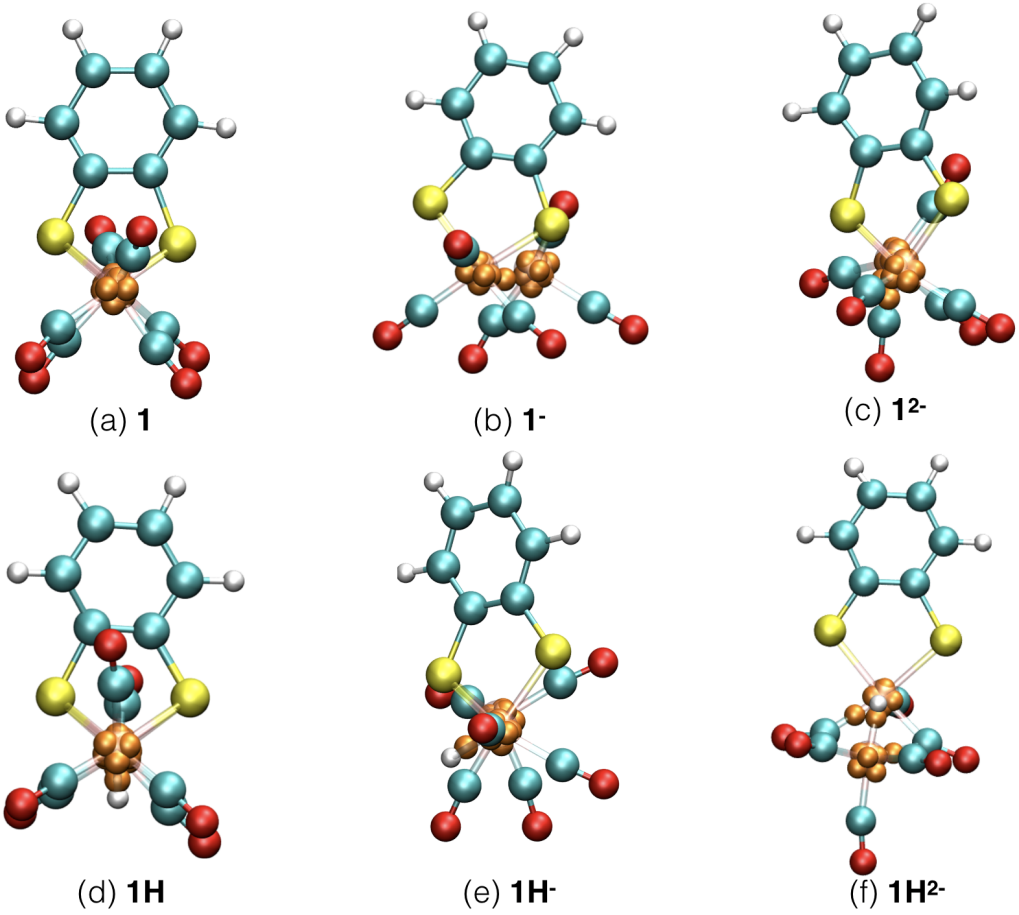

Figure 6: Side view of all intermediate complexes.

5 pK_a calculation of complex 1^-

Constrained molecular dynamics simulations were carried out to calculate the pK_a of the $\mathbf{1}^-$ complex. The distance between the hydrogen and the donating acetonitrile nitrogen atoms was taken as the reaction coordinate and constrained at different values in a series of nine constrained DFT-MD runs. At the largest N-H distance, the bridging hydride moiety is formed. Figure 7 shows snapshots from each of these runs. See the main text for the resulting free energy profile and the computed pK_a value. Tables 9 and 10 show the average Fe-H bond lengths in each of the constrained DFT-MD runs.

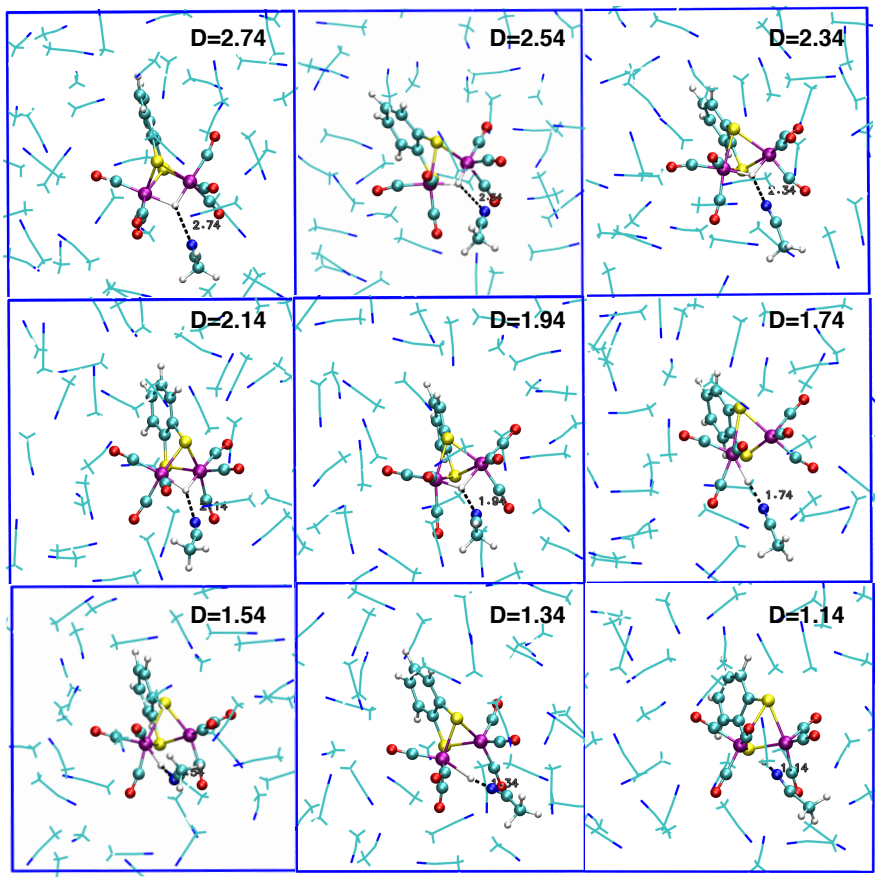

Figure 7: Snapshots from the nine constrained DFT-MD simulations. The indicated D is the constrained N-H distance in Å.

Bond	Bond Length in Å								
N-H	2.74	2.54	2.34	2.14	1.94	1.74	1.54	1.34	1.14
Fe1-H	1.70	1.72	1.73	1.75	1.80	2.21	2.3	2.25	2.48
Fe2-H	1.70	1.70	1.73	1.75	1.78	3.5	3.25	3.23	3.22

Table 9: Average Fe-H bond lengths in each of the constrained DFT-MD simulations, in which the N-H bond length (top row) is fixed to obtain the free energy for the protonation reaction $\mathbf{1}^- + \mathbf{H}^+ \rightarrow \mathbf{1H}$.

Bond	Bond Length in Å								
N-H	2.9	2.6	2.3	2.0	1.7	1.4	1.3	1.2	1.1
Fe1-H	1.83	1.85	1.89	2.59	2.44	2.67	2.91	2.74	3.17
Fe2-H	1.62	1.63	1.63	1.60	1.64	1.80	2.1	2.05	3.57

Table 10: Average Fe-H bond lengths in each of the constrained DFT-MD simulations, in which the N-H bond length (top row) is fixed to obtain the free energy for the protonation reaction $\mathbf{1}^{2-} + \mathbf{H}^{+} \rightarrow \mathbf{1H}^{-}$.

6 Metadynamics collective variables

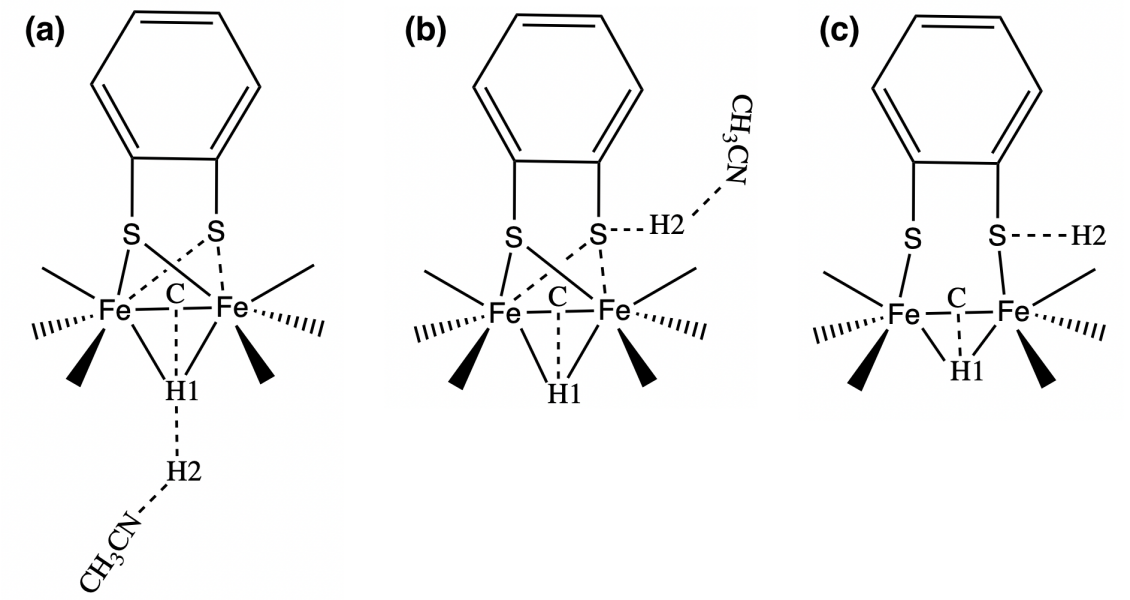

Figure 8: Atom labeling to illustrate the collective variables used in the three metadynamics simulations. (a) Collective variables used in the direct protonation of bridging hydride (Fig.10 in the main text). (b) Collective variables used in the protonation of the sulfur (Fig.11 in the main text). (c) Collective variables used in the second step (Fig.12 in the main text). C is the center of mass of the two Fe atoms.

References

[1] G. A. N. Felton, A. K. Vannucci, J. Chen, L. T. Lockett, N. Okumura, B. J. Petro, U. I. Zakai, D. H. Evans, R. S. Glass and D. L. Lichtenberger, *J. Am. Chem. Soc.*, 2007, **129**, 12521–12530.

[2] N. Leidel, C.-H. Hsieh, P. Chernev, K. G. V. Sigfridsson, M. Y. Darensbourg and M. Haumann, *Dalton Trans.*, 2013, **42**, 7539–7554.

[3] M. Etinski, I. M. Stanković, R. C. Puthenkalathil and B. Ensing, *New J. Chem.*, 2020, **44**, 932–941.